Biophysical Journal Volume 76 March 1999 1293–1309

Kinetic and Thermodynamic Aspects of Lipid Translocation in Biological Membranes

Stephan Frickenhaus and Reinhart Heinrich
Humboldt University Berlin, Institute of Biology and Theoretical Biophysics, D-10115 Berlin, Germany

ABSTRACT A theoretical analysis of the lipid translocation in cellular bilayer membranes is presented. We focus on an integrative model of active and passive transport processes determining the asymmetrical distribution of the major lipid components between the monolayers. The active translocation of the aminophospholipids phosphatidylserine and phosphatidylethanolamine is mathematically described by kinetic equations resulting from a realistic ATP-dependent transport mechanism. Concerning the passive transport of the aminophospholipids as well as of phosphatidylcholine, sphingomyelin, and cholesterol, two different approaches are used. The first treatment makes use of thermodynamic flux-force relationships. Relevant forces are transversal concentration differences of the lipids as well as differences in the mechanical states of the monolayers due to lateral compressions. Both forces, originating primarily from the operation of an aminophospholipid translocase, are expressed as functions of the lipid compositions of the two monolayers. In the case of mechanical forces, lipid-specific parameters such as different molecular surface areas and compression force constants are taken into account. Using invariance principles, it is shown how the phenomenological coefficients depend on the total lipid amounts. In a second approach, passive transport is analyzed in terms of kinetic mechanisms of carrier-mediated translocation, where mechanical effects are incorporated into the translocation rate constants. The thermodynamic as well as the kinetic approach are applied to simulate the time-dependent redistribution of the lipid components in human red blood cells. In the thermodynamic model the steady-state asymmetrical lipid distribution of erythrocyte membranes is simulated well under certain parameter restrictions: 1) the time scales of uncoupled passive transbilayer movement must be different among the lipid species; 2) positive cross-couplings of the passive lipid fluxes are needed, which, however, may be chosen lipid-unspecifically. A comparison of the thermodynamic and the kinetic approaches reveals that antiport mechanisms for passive lipid movements may be excluded. Simulations with kinetic symport mechanisms are in qualitative agreement with experimental data but show discrepancies in the asymmetrical distribution for sphingomyelin.

INTRODUCTION

Plasma membranes of eukaryotic cells show a pronounced asymmetry with respect to the distributions of the major lipid components among the two monolayers. The aminophospholipids phosphatidylserine (PS) and phosphatidylethanolamine (PE) are predominantly located on the cytoplasmic leaflet, whereas the phospholipids phosphatidylcholine (PC) and sphingomyelin (SM) are mainly found on the external leaflet (Bretscher, 1972; Verkleij et al., 1973; Gordesky and Marinetti, 1973; cf. Devaux, 1991; Zachowski, 1993). Evidence of the distribution of cholesterol (Ch) as another membrane component is still contradictory. Some authors found for cholesterol a preference for the cytoplasmic layer of the red blood cell membrane (Brasaemle et al., 1988; Schroeder et al., 1991), whereas other results indicate a rather symmetrical distribution (Blau and Bittman, 1978; Lange and Slayton, 1982).

As has been demonstrated by Seigneuret and Devaux (1984), the asymmetrical distribution of the aminophospholipids may be understood by an ATP-dependent translocation of these components from the external to the cytoplasmic layer. The response of the membrane to this directed transport will concern not only the counter-directed movement of PS and PE, but also a redistribution of PC, SM, and Ch. Furthermore, a change in membrane curvature may occur because of geometrical restrictions and corresponding mechanical forces caused by the coupling of the monolayer surfaces. This reasoning shows that the membrane asymmetry is determined by a multitude of processes, depending on 1) the metabolic state of the cell, 2) the mechanism of active translocation, 3) the transmembrane concentration differences of lipids, and 4) mechanical forces.

Obviously, the interaction of different translocation processes may be adequately described only on the basis of biophysical models allowing quantitative estimates for different experimental situations under time-independent and time-dependent conditions. Mathematical models of molecular mechanisms of lipid translocation are still rare. Previous investigations (Brumen et al., 1993; Heinrich et al., 1997) indicated that an explanation of the asymmetrical molecular composition of bilayers needs to consider free energy contributions from mixing entropy as well as from mechanical effects of lateral compressions. However, in the work of Brumen et al. (1993), the expressions for fluxes resulting from mechanical stress, the so-called compensatory fluxes, are not well defined in their physical meaning. A drawback of the paper of Heinrich et al. (1997) is that the

Received for publication 9 February 1998 and in final form 8 September 1998.

Address reprint requests to Reinhart Heinrich, Institute of Biology and Theoretical Biophysics, Humboldt University Berlin, Invalidenstrasse 42, 10115 Berlin, Germany. Tel.: 49-30-20938698; Fax: 49-30-20938813; E-mail: reinhart-heinrich@rz.hu-berlin.de.

0006-3495/99/03/1293/17 $2.00

use of monolayer mixing entropy is not fully justified for two coupled monolayers. Furthermore, the latter analysis assumes that the mechanical properties of the lipids are species independent, which is an oversimplification, at least for cholesterol.

Correct theoretical investigations of the membrane on a microscopic level are crucial for understanding macroscopic cellular phenomena such as shapes of cells. In the latter field of research much theoretical work has been done using methods of elasticity theory (see Svetina and Žekš, 1989; Seifert et al., 1991; Heinrich et al., 1993). Membrane properties such as spontaneous curvature and relative area changes of the monolayers, which enter the shape-determining energy functional, should be directly related to the asymmetrical composition of the bilayer.

This study is intended to gain a more complete understanding of the phenomena of transbilayer lipid movement by finding an appropriate phenomenological description of the lipid fluxes. The steady-state asymmetrical lipid distribution is governed by dynamics equations. A reference simulation with a minimal set of phenomenological parameters yields qualitative restrictions to the many possible translocation mechanisms. Relations between phenomenological and kinetic model parameters serve, furthermore, as guidelines for the selection of kinetic constants in a quantitative way. It is shown how the mechanical driving forces of the phenomenological model are to be incorporated into a kinetic model of lipid translocation.

BASIC MODEL ASSUMPTIONS

Let us consider a bilayer membrane of one cell composed of s different lipids, which are subject to translocation processes between the cytoplasmic monolayer c and the external monolayer e. The amounts, in units of moles per cell, of the lipids i, $i = 1, \ldots, s$, on the monolayers are denoted by N_i^c and N_i^e. They are related to the differences $n_i = N_i^c - N_i^e$ and to the total amounts of lipids $N_i = N_i^c + N_i^e$ as follows:

$$N_i^c = \frac{N_i + n_i}{2}, \quad N_i^e = \frac{N_i - n_i}{2}. \tag{1}$$

The time-dependent changes of the composition of the monolayers are governed by the differential equations

$$\frac{dN_i^c}{dt} = -\frac{dN_i^e}{dt} = J_i^{act} + J_i^{pass}, \tag{2}$$

where J_i^{act} and J_i^{pass} denote the fluxes of active and passive transport, respectively. Fluxes have positive sign if lipid amounts on the cytoplasmic side are increased. In this equation it is assumed that the total amount N_i is constant, that is, the model does neither include insertions of the lipids into the membrane or extractions of the lipids from the membrane. Lipids are considered to be distributed homogeneously in lateral directions. Furthermore, there is no intermediate state at the transport of the lipids from one leaflet to the other.

For the fluxes J_i^{act} we use an ATP-dependent carrier mechanism as described previously (Heinrich et al., 1997; cf. also Simulations). Passive fluxes are described first in the framework of linear irreversible thermodynamics, and second on the basis of kinetic translocation models.

In the thermodynamic approach we apply linear flux-force relationships,

$$J_i^{pass} = \sum_j L_{ij} X_j, \tag{3}$$

where X_j denotes thermodynamic forces. The coefficients L_{ij} are referred to as phenomenological coefficients and are assumed to be state independent, i.e., they have constant values in time. They may depend, however, on system parameters such as total lipid amounts and lipid-specific molecular parameters. For the forces X_j we analyze in the following sections entropic effects and mechanical effects within lipid bilayers. Both types of forces may be expressed as functions of the variables N_i^c or N_i^e and of lipid-specific parameters. Gradients in temperature are neglected, that is, the solvent on both sides of the membrane acts as a heat bath.

In the kinetic approach it is assumed that passive diffusion fluxes of lipids are mediated by a protein carrier. Two different mechanisms are analyzed: first, an antiport mechanism, and second, a symport mechanism. Near equilibrium the linearized kinetic equations may be directly compared to the phenomenological equations of the thermodynamic approach. In this way the coupling coefficients may be expressed in terms of the kinetic parameters of the carrier.

PHENOMENOLOGICAL FORCES OF THE LATERAL IDEALLY MIXING BILAYER

Entropic forces

The free energy F of the bilayer can be derived from combinatorial considerations under the following assumptions: 1) ideal mixing of the lipids within both monolayers (i.e., non-lipid-specific interactions), 2) negligible molecular transbilayer interactions, and 3) no internal degrees of freedom for the conformation of the lipid molecules. Hence F is related to a configurational partition function Z by $F = -k_B T \ln Z$, where k_B is Boltzmann's constant. The partition function may be calculated from the macroscopic configurations of a bilayer, which are characterized by the numbers of lipid molecules $\Lambda_i^c = L_A N_i^c$ and $\Lambda_i^e = L_A N_i^e$ of species i on either monolayer, e or c, respectively. L_A denotes Avogadro's number.

The configurational partition function of the bilayer reads

$$Z = \prod_{i=1}^{s} \frac{\Lambda_i!}{\Lambda_i^c! \Lambda_i^e!}. \tag{4}$$

Z takes into account the number of microscopic distributions of Λ_i molecules of each lipid species among the

monolayers with a lipid number Λ_i^c and Λ_i^e on the two layers.

The entropic contribution to the total free energy (in Joules) of a single membrane reads

$$F = -k_B T \ln Z. \tag{6}$$

Using Stirling's formula, $\ln x! \approx x \ln x - x$ for $x \gg 1$, one derives from Eqs. 4–6

$$\frac{F}{k_B T} = -\sum_j \Lambda_j \ln \Lambda_j + \sum_j (\Lambda_j^c \ln \Lambda_j^c + \Lambda_j^e \ln \Lambda_j^e). \tag{7}$$

It is easy to see that at variations of Λ_j^c and Λ_j^e under the constraint $\Lambda_j = \Lambda_j^c + \Lambda_j^e$ = constant, the free energy attains its minimum for an equal distribution of each lipid species among the two monolayers. In terms of molar amounts the equilibrium state is, therefore, characterized by

$$N_i^c = N_i^e = \frac{N_i}{2}. \tag{8}$$

Nonequilibrium states are characterized by the variables

$$y_i = N_i^c - \frac{N_i}{2} = -N_i^e + \frac{N_i}{2}, \tag{9}$$

which are related to the differences $n_i = N_i^c - N_i^e$ by $n_i = 2y_i$. Defining entropic forces in units of J/mol as

$$X_i^{entr} = -\frac{\partial F}{\partial y_i}, \tag{10}$$

one derives

$$X_i^{entr} = -RT \ln \frac{N_i^c}{N_i^e}. \tag{11}$$

This formula for the entropic force shows some correspondence to an expression used in a previous study (Heinrich et al., 1997). However, in the latter work entropic forces have been expressed from differences of lateral mixing entropies between the monolayers, which would be a correct treatment if the monolayers were allowed to uncouple in their surface areas.

For small deviations from the equilibrium state ($n_i \ll N_i$) the entropic forces may be expressed in a linear approximation as

$$X_i^{entr} = -2RT \frac{n_i}{N_i}. \tag{12}$$

Mechanical forces

Changes in the lipid compositions of the monolayers caused by passive or active translocation will affect the mechanical energy of the membrane because of changes in lateral distances between the molecules. For small deviations from equilibrium, the lateral mechanical energies of the two monolayers c and e may be expressed in a harmonic approximation as

$$E^{c,e} = \tfrac{1}{2} \sum_i \gamma_i a_i N_i^{c,e} (\xi_i^{c,e})^2, \tag{13}$$

where a_i and $\xi_i^{c,e}$ denote, for lipid species i, the equilibrium membrane surface area per molecule, and the area change relative to the equilibrium area on the two layers, respectively. γ_i represents the force constant per unit area. In Eq. 13 the relative area changes are assumed to be equal for all molecules of one species i, but different in each monolayer, that is, the tension in the monolayer is distributed homogeneously over the molecules of each species. Furthermore, equilibrium areas and force constants are considered to be layer independent.

Because the two monolayers are coupled in such a way that there is a common closed contact surface within the membrane, the surface area of the cytoplasmic layer and that of the external layer cannot vary independently (cf. the bilayer couple hypothesis of Sheetz and Singer, 1974). In particular, one expects that the surface areas of lipids located in the monolayer with increased amounts will be compressed, whereas the areas of lipids within the other monolayer will be expanded. Thus the relative changes $\xi_i^{c,e}$ of areas will depend on the deviations n_i characterizing the nonequilibrium state of the membrane. To derive the corresponding relation, one may assume in a first approximation that, under deviation from equilibrium, the total surface areas of each layer remain unchanged, that is,

$$A^{c,e}(\xi_i^{c,e}, n_i) = A_0^{c,e}, \tag{14}$$

where $A_0^{c,e}$ are the total equilibrium surfaces of the monolayers. In nonequilibrium states the two areas may be expressed as

$$A^{c,e}(\xi_i^{c,e}, n_i) = \tfrac{1}{2} \sum_j (N_j \pm n_j) a_j (1 + \xi_i^{c,e}). \tag{15}$$

The term $a_j(1 + \xi_j^{c,e})$ represents the compressed ($\xi < 0$) or expanded ($\xi > 0$) area of lipid j in layer c and e, respectively. From Eq. 15 it follows with condition 14 that

$$\sum_j N_j a_j = \sum_j (N_j \pm n_j) a_j (1 + \xi_i^{c,e}). \tag{16}$$

In this equation it is assumed that $A_0^c = A_0^e = A_0$, i.e., the membrane is symmetrical at equilibrium (for a more general ansatz see the Discussion). In a previous study (cf. Heinrich et al., 1997) relation 16 was used to calculate the relative area changes under the assumption $\xi_j^c = -\xi_j^e = \xi$, that is, they are identical for all lipids. Such a simplification may not be justified for lipid species of different equilibrium areas a_i and of different force constants γ_i. Accordingly, further relations must be taken into account besides Eq. 16 to calculate the individual area changes. Such relations may be obtained by considering the elastic energy of each monolayer to be at minimum. This assumption is supported by the fact that, after perturbation of the equilibrium state, relax-

ation of the mechanical stress on both monolayers will occur on a much shorter time scale than transversal redistribution of lipids. This mechanical relaxation will be supported, for example, by the fast lateral redistribution of lipids. Minimization of this energy under the constraints in Eq. 16 can be performed with two Lagrange multipliers v^c and v^e. With

$$E^* = E^c + E^e + v^c[A^c(\xi_i^c) - A_0] + v^e[A^e(\xi_i^e) - A_0], \quad (17)$$

the lateral elastic energy of the bilayer has an extremum if

$$\frac{\partial E^*}{\partial \xi_i^c} = 0, \quad \frac{\partial E^*}{\partial \xi_i^e} = 0. \quad (18a,b)$$

From Eqs. 13, 15, 17, and 18 one obtains

$$\gamma_i a_i N_i^{c,e} \xi_i^{c,e} + \tfrac{1}{2} v^{c,e}(N_i \pm n_i)a_i = 0, \quad (19)$$

which under consideration of Eq. 1 yields

$$\xi_i^{c,e} = -\frac{v^{c,e}}{\gamma_i}. \quad (20)$$

By taking into account the constraints in 16 in Eq. 20, one derives

$$\xi_i^{c,e} = \mp \frac{(1/\gamma_i)\sum_j n_j a_j}{\sum_k (N_k \pm n_k)a_k/\gamma_k}. \quad (21)$$

For sufficiently small deviations from equilibrium, the linear approximation

$$\xi_i^{c,e} = \mp \frac{(1/\gamma_i)\sum_j n_j a_j}{\sum_k N_k a_k/\gamma_k} \quad (22)$$

is valid. The total mechanical energy $E = E^c + E^e$, obtained by introducing relation 22 into Eq. 13, reads

$$E = \frac{1}{2\sum_k N_k a_k/\gamma_k}\left(\sum_j n_j a_j\right)^2, \quad (23)$$

where terms higher than second order are neglected.

The mechanical forces are defined as

$$X_i^{mech} = -\frac{\partial E}{\partial y_i} \quad (24)$$

(see the definition of the entropic forces in Eq. 10). From Eqs. 23 and 24 one obtains with $n_i = 2y_i$

$$X_i^{mech} = -\frac{2a_i \sum_j n_j a_j}{\sum_k N_k a_k/\gamma_k}. \quad (25)$$

It is worth mentioning that in the special case of unspecific parameters ($\gamma_i = \gamma$, $a_i = a$), Eqs. 22 and 25 reduce to previously derived expressions (cf. Heinrich et al., 1997). As expected, all mechanical forces are reduced in the presence of lipid species that are soft with respect to lateral area changes, i.e., species that have a low γ value. Equation 25 reveals that forces are related pairwise by $X_i^{mech}/X_j^{mech} = a_i/a_j$. Furthermore, all forces are proportional to

$$\Delta A = \sum_j n_j a_j, \quad (26)$$

which may be considered as the area difference of *uncoupled* monolayers.

In the following we combine the entropic force and the mechanical force as the total force of passive translocation:

$$X_i = X_i^{entr} + X_i^{mech}. \quad (27)$$

The equilibrium state where the total energy $F + E$ has its minimum is characterized by a symmetrical distribution of each lipid component among the monolayers ($n_i = 0$).

PHENOMENOLOGICAL COEFFICIENTS FOR PASSIVE TRANSLOCATIONS

Parameterization with respect to lipid amounts

In Eq. 3 the phenomenological coefficients L_{ij} are unknown. A certain knowledge concerning the dependence of L_{ij} on molecular membrane parameters may be obtained on the basis of special kinetic models (see below). Furthermore, these coefficients may be fitted to experimental data. More generally, one may apply invariance principles to derive various restrictions for the structure of these coefficients, particularly concerning their dependencies on the total amounts of lipids. We use the principle that macroscopically the behavior of the system should be independent of a decomposition of a certain lipid species into two identical subspecies.

Let us consider an arbitrary decomposition of a certain species k into two subspecies a and b, such that their total amounts N_a and N_b and the deviations from equilibrium n_a and n_b are related to the corresponding quantities of species k as follows:

$$N_a = (\tfrac{1}{2} + \epsilon)N_k, \quad N_b = (\tfrac{1}{2} - \epsilon)N_k, \quad (28a,b)$$

$$n_a = (\tfrac{1}{2} + \epsilon)n_k, \quad n_b = (\tfrac{1}{2} - \epsilon)n_k. \quad (28c,d)$$

The parameter ϵ that quantifies the decomposition of species k is confined by $-1/2 \le \epsilon \le 1/2$. It follows directly from Eqs. 1, 12, and 25 that the forces of species a and b are the same as the force of species k:

$$X_a = X_b = X_k. \quad (29)$$

For fixed k, the linear flux-force relations in Eq. 3 may be rewritten for the original system as

$$J_k = L_{kk}X_k + \sum_{j\neq k} L_{kj}X_j, \quad (30a)$$

$$J_{i\neq k} = \sum_{j\neq k} L_{ij}X_j + L_{ik}X_k. \quad (30b)$$

Characterizing the quantities of the decomposed system by the superscript * gives

$$J^*_a + J^*_b = L^*_{aa}X_a + L^*_{ab}X_b + L^*_{bb}X_b + L^*_{ba}X_a + \sum_{j\neq a,b}(L^*_{aj} + L^*_{bj})X_j, \tag{31a}$$

$$J^*_{i\neq a,b} = \sum_{j\neq a,b} L^*_{ij}X_j + L^*_{ia}X_a + L^*_{ib}X_b. \tag{31b}$$

Obviously, the macroscopic properties of the membrane, particularly the passive translocation fluxes, should be invariant with respect to the decomposition in Eq. 28, that is,

$$J_k = J^*_a + J^*_b, \quad J_{i\neq k} = J^*_{i\neq a,b}. \tag{32a,b}$$

The deviations n_i from equilibrium and, therefore, the forces X_i may vary independently. Thus, taking into account Eqs. 30 and 31 in Eq. 32, and using Onsager's reciprocity relation $L_{ij} = L_{ji}$, one derives that the phenomenological coefficients have to fulfill the relations

$$L^*_{ij} = L_{ij} \quad \text{for } i,j \neq a, b, k \tag{33a}$$

$$L^*_{ia} + L^*_{ib} = L_{ik} \quad \text{for } i \neq a, b, k \tag{33b}$$

$$L^*_{aa} + L^*_{bb} + 2L^*_{ab} = L_{kk}. \tag{33c}$$

To derive dependencies of the phenomenological coefficients on the lipid amounts, the following ansatz is used:

$$L_{ij} = \frac{\lambda_{ij}}{2}(N^x_i N^y_j + N^y_i N^x_j), \quad i,j = 1,\ldots,s, \tag{34a}$$

$$L^*_{ij} = \frac{\lambda^*_{ij}}{2}(N^x_i N^y_j + N^y_i N^x_j), \quad i,j = 1,\ldots,k-1,a,b, k+1,\ldots,s. \tag{34b}$$

The parameters λ_{ij} and λ^*_{ij}, which must be components of a symmetrical matrix, do not contain any further factors of N_i and N_j, but possibly factors N_l with $l \neq i, j$. Constraints on further relations for the dependencies of the parameters λ_{ij} on the total lipid amounts are given below (see Eq. 44a,b). The values of the exponents x and y have to be determined from the invariance properties mentioned above. Inserting Eqs. 34a,b into Eq. 33b gives, together with the decomposition 28a,b,

$$\frac{\lambda^*_{ia}}{2}\left(\left(\frac{1}{2}+\epsilon\right)^y N^x_i N^y_k + \left(\frac{1}{2}+\epsilon\right)^x N^y_i N^x_k\right) + \frac{\lambda^*_{ib}}{2}\left(\left(\frac{1}{2}-\epsilon\right)^y N^x_i N^y_k + \left(\frac{1}{2}-\epsilon\right)^x N^y_i N^x_k\right) = \frac{\lambda_{ik}}{2}(N^x_i N^y_k + N^y_i N^x_k). \tag{35}$$

Because species a, b, and k have the same physical properties, their parameters λ will be identical:

$$\lambda^*_{ia} = \lambda^*_{ib} = \lambda_{ik}. \tag{36}$$

Furthermore, Eq. 35 must be valid for any decomposition of species k, that is, the left-hand side should be independent of ϵ. For $x = y$, Eq. 35 reads, considering Eq. 36,

$$(\tfrac{1}{2}+\epsilon)^z + (\tfrac{1}{2}-\epsilon)^z = 1, \tag{37a}$$

where $z = x = y$. This equation is independent of ϵ only for $z = 1$. For $x \neq y$ two separate conditions are obtained:

$$(\tfrac{1}{2}+\epsilon)^x + (\tfrac{1}{2}-\epsilon)^x = 1, \quad (\tfrac{1}{2}+\epsilon)^y + (\tfrac{1}{2}-\epsilon)^y = 1, \tag{37b,c}$$

since Eq. 35 holds for arbitrary values of both amounts N_i and N_k. Obviously these two equations (37b,c) cannot be fulfilled simultaneously for $x \neq y$ and arbitrary ϵ. Thus we are left with the only possibility, $x = 1$ and $y = 1$. Using this result, we obtain from Eq. 34a for the cross-coupling coefficients

$$L_{ik} = \lambda_{ik}N_iN_k \quad \text{for } i \neq k. \tag{38}$$

To find expressions for the diagonal elements L_{kk}, we use relation 34a,b in Eq. 33c and take into account Eq. 38. This yields

$$\lambda^*_{aa}(\tfrac{1}{2}+\epsilon)^{x+y} + \lambda^*_{bb}(\tfrac{1}{2}-\epsilon)^{x+y} + 2\lambda^*_{ab}(\tfrac{1}{2}+\epsilon)(\tfrac{1}{2}-\epsilon) = \lambda_{kk}. \tag{39}$$

Because $\lambda^*_{aa} = \lambda^*_{bb} = \lambda_{kk}$, Eq. 39 gives

$$\lambda_{kk}((\tfrac{1}{2}+\epsilon)^z + (\tfrac{1}{2}-\epsilon)^z) + 2\lambda^*_{ab}(\tfrac{1}{4}-\epsilon^2) = \lambda_{kk}, \tag{40}$$

where $z = x + y$. For z there are two solutions such that Eq. 40 is independent of ϵ. The first solution reads $z = 1$, with $\lambda^*_{ab} = 0$, and arbitrary values of λ_{kk} denoted in the following κ_k. The second solution reads $z = 2$, for which Eq. 40 holds independent of ϵ only with $\lambda_{kk} = \lambda^*_{ab}$. Linear combination of these two solutions yields for the diagonal elements

$$L_{kk} = \kappa_kN_k + \lambda_{kk}N^2_k. \tag{41}$$

This expression shows that the diagonal elements L_{kk} are composed of a diffusion term κ_kN_k and a self-coupling term $\lambda_{kk}N^2_k$.

Combining relations 38 and 41, one obtains the following general expression for the phenomenological coefficients:

$$L_{ij} = \delta_{ij}\kappa_jN_j + \lambda_{ij}N_iN_j. \tag{42}$$

Concerning the parameters entering the phenomenological coefficients in Eq. 42, we use the notation diffusion parameters κ_i, self-coupling parameters λ_{ii}, and cross-coupling parameters λ_{ij} for $i \neq j$.

Under the assumption of a lateral homogeneous membrane, two general properties of the diffusion parameters κ_j and coupling parameters λ_{ij} that enter Eq. 42 can be derived. For any subsection of the bilayer characterized by $N'_k = \alpha N_k$ and $n'_k = \alpha n_k$ for $k = 1,\ldots,s$ with a scaling parameter α, confined to $0 < \alpha \leq 1$, the following relations should be

fulfilled:

$$\alpha J_i(N_1, \ldots, N_s, n_1, \ldots, n_s) = J_i(\alpha N_1, \ldots, \alpha N_s, \alpha n_1, \ldots, \alpha n_s) \quad (43a)$$

$$X_i(N_1, \ldots, N_s, n_1, \ldots, n_s) = X_i(\alpha N_1, \ldots, \alpha N_s, \alpha n_1, \ldots, \alpha n_s), \quad (43b)$$

that is, the fluxes and forces are homogeneous functions in the amounts of lipids of first degree and degree zero, respectively. Applying the linear flux-force relations to these subsections of the membrane, one obtains that the phenomenological coefficients are homogeneous functions of first degree in the lipid amounts. Taking into account expression 42, one obtains that κ_i is homogeneous of degree zero and λ_{ij} of degree -1, respectively. Accordingly, one derives from Euler's theorem on homogeneous functions the following conditions:

$$\sum_k \frac{\partial \kappa_i}{\partial N_k}\frac{N_k}{\kappa_i} = 0, \quad \sum_k \frac{\partial \lambda_{ij}}{\partial N_k}\frac{N_k}{\lambda_{ij}} = -1. \quad (44a,b)$$

In the most simple case, Eq. 44a is fulfilled if all diffusion parameters are independent of the lipid amounts, whereas Eq. 44b is fulfilled if all coupling parameters are proportional to the inverse of the total lipid amount.

Taking into account result 42, the passive translocation fluxes, defined in Eq. 3, read

$$J_i^{pass} = -\sum_j(\kappa_j\delta_{ij}N_j + \lambda_{ij}N_iN_j)\left(RT\ln\left(\frac{N_j + n_j}{N_j - n_j}\right) + \frac{2a_j\sum_k n_ka_k}{\sum_k N_ka_k/\gamma_k}\right). \quad (45)$$

For the simulation of lipid translocation this flux equation may be used in Eq. 3.

Parameterization with respect to membrane surface areas of lipids

In this subsection we show that the coupling parameters λ_{ij} in Eq. 42 may be related to the equilibrium surface areas a_i of the lipids, which, besides the lipid amounts, are the relevant parameters of the present model. Let us consider a certain lipid species, say k, and a perturbation from the equilibrium state such that

$$n_k = 0, \quad \sum_i n_ia_i = 0. \quad (46a,b)$$

Equation 46a entails that the entropic force in Eq. 12 of species k vanishes, whereas Eq. 46b implies that no mechanical forces occur (see Eq. 25). If there are no lipid-specific interactions, one may conclude that all states fulfilling Eq. 46a,b are characterized by a vanishing passive flux of species k, which yields, using Eqs. 3 and 12, in the vicinity of equilibrium,

$$\sum_{j\neq k} L_{kj}\frac{n_j}{N_j} = 0. \quad (47)$$

Taking into account the general structure for the nondiagonal elements L_{kj} given in Eq. 42, one derives from Eq. 47 the following condition for the cross-coupling parameters:

$$N_k\sum_{j\neq k}\lambda_{kj}n_j = 0. \quad (48a)$$

Equation 48a states that a vector $\vec{l}^k = (\lambda_{k1} \cdots \lambda_{k,k-1}\ \lambda_{k,k+1} \cdots \lambda_{ks})^T$ is orthogonal to any vector of perturbations $\vec{n}^k = (n_1 \cdots n_{k-1}\ n_{k+1} \cdots n_s)^T$, which in vector notation reads

$$\vec{l}^k \cdot \vec{n}^k = 0. \quad (48b)$$

The space of perturbations $\vec{n}^k$ restricted by Eqs. 46a,b is of dimension $s - 2$. Accordingly, this space is spanned by $s - 2$ vectors $\vec{b}^{(i,k)}$ ($i = 1, \ldots, s - 2$). In the case $k = s$, for example, a special choice of these vectors reads

$$\vec{b}^{(1,s)} = \begin{pmatrix} a_2 \\ -a_1 \\ 0 \\ 0 \\ \vdots \\ 0 \end{pmatrix}, \quad \vec{b}^{(2,s)} = \begin{pmatrix} 0 \\ a_3 \\ -a_2 \\ 0 \\ \vdots \\ 0 \end{pmatrix}, \ldots, \quad \vec{b}^{(s-2,s)} = \begin{pmatrix} 0 \\ \vdots \\ 0 \\ 0 \\ a_{s-1} \\ -a_{s-2} \end{pmatrix}. \quad (49)$$

Generally, the elements of the vector $\vec{b}^{(i,s)}$ are given by $b_j^{(i,s)} = 0$ for $1 \le j \le i - 1$ and $i + 2 \le j \le s - 1$, and $b_i^{(i,s)} = a_{i+1}$, $b_{i+1}^{(i,s)} = -a_i$. Similar representations are obtained for $k \neq s$.

The condition 48b of orthogonality is fulfilled if $\vec{l}^k$ is orthogonal to all corresponding vectors $\vec{b}^{(i,k)}$, which yields

$$\vec{l}^k \cdot \vec{b}^{(i,k)} = 0 \quad \text{for } i = 1, \ldots, s - 2. \quad (50)$$

It can be shown that there is one parameter v_k, such that Eq. 50 is fulfilled with

$$\lambda_{kj} = v_ka_j \quad \text{with } k, j = 1, \ldots, s \text{ and } k \neq j. \quad (51)$$

For $k = s$ this result may be easily verified by using Eq. 49. The symmetry relations $\lambda_{kj} = \lambda_{jk}$ require $v_ka_j = v_ja_k$, which leads to

$$\lambda_{kj} = va_ja_k. \quad (52)$$

The combination of Eqs. 42 and 52 gives

$$L_{ij} = \delta_{ij}\kappa_jN_j + va_ia_jN_iN_j. \quad (53)$$

According to this equation, the $s(s + 1)/2$ phenomenological coefficients L_{ij} are fixed by only $s + 1$ phenomenological parameters v and κ_j. Relation 53 may be used also for the case of equal lipid area parameters, that is, for $a_j = a$.

The requirement for the matrix L_{ij} to be positive definite (see de Groot and Mazur, 1962) sets a certain limit for the unknown parameter v. For example, any choice of v must

ensure that the diagonal elements L_{ii} are positive. Thus there is a lower limit for v depending on the values of $\kappa_i > 0$ and $a_i > 0$.

Phenomenological coefficients as derived from kinetic models

On the phenomenological level of description, the parameters κ_j and λ_{ij} in Eq. 42 and, similarly, the parameter v in Eq. 52 have no mechanistic interpretation. In this section we consider the case in which lipid translocation is mediated by a carrier protein. This allows us to express the phenomenological parameters in terms of kinetic constants.

Kinetic models without mechanical effects

Antiport mechanism. Let us assume that the translocation carrier has only one binding site, to which the lipids bind in a competitive way. If this binding is fast compared to translocation, the following equilibrium relations hold:

$$\frac{P_i^{c,e}}{P^{c,e} \cdot N_i^{c,e}} = K_i^{c,e}, \quad i = 1, \ldots, s, \tag{54}$$

where $P_i^{c,e}$ and $P^{c,e}$ denote the amounts of the loaded forms and of the unloaded forms, respectively. In this equation $N_i^{c,e}$ are the amounts of free lipids, that is, lipids not bound to the carrier. We assume that the total amount of loaded carrier forms is much smaller compared to the individual lipid amounts such that $N_i = N_i^c + N_i^e$ holds true. Conservation of the total amount P of carrier molecules leads with Eq. 54 to the relation

$$P = P^c\left(1 + \sum_i K_i N_i^c\right) + P^e\left(1 + \sum_i K_i N_i^e\right). \tag{55}$$

A quasi-steady-state approximation for the distribution of the carrier among the two layers yields

$$\sum_i l_i^+ P_i^c + k^+ P^c = \sum_i l_i^- P_i^e + k^- P^e, \tag{56}$$

where l_i^+ and l_i^- denote the translocation rate constants of the loaded carrier forms, and k^+ and k^- denote the rate constants of movement of the unloaded carrier forms. One obtains with the help of Eqs. 54–56

$$P^c = \frac{P \cdot B^e}{A^c B^e + A^e B^c}, \quad P^e = \frac{P \cdot B^c}{A^c B^e + A^e B^c}, \tag{57a,b}$$

with

$$A^{c,e} = 1 + \sum_i K_i N_i^{c,e}, \quad B^{c,e} = k^{+,-} + \sum_i l_i^{+,-} K_i N_i^{c,e}. \tag{58a,b}$$

Because the time-dependent changes of the lipid amounts are characterized by

$$\frac{d}{dt}(N_i^c + P_i^c) = -\frac{d}{dt}(N_i^e + P_i^e) = l_i^- P_i^e - l_i^+ P_i^c, \tag{59}$$

one obtains from Eqs. 54 and 57

$$\frac{dN_i^c}{dt} = -\frac{dN_i^e}{dt} = \frac{K_i P(l_i^- N_i^e B^c - l_i^+ N_i^c B^e)}{A^c B^e + A^e B^c}, \tag{60}$$

where again $P_i^{c,e} \ll N_i^{c,e}$ is assumed (see Schultz, 1980).

To express the coupling parameters in terms of kinetic constants, Eq. 60 has to be applied for states near equilibrium. In the case characterized by $K_i^c = K_i^e = K_i$, $l_i^+ = l_i^- = l_i$ and $k^+ = k^- = k$ (symmetrical carrier), the equilibrium amounts are $N_i^c = N_i^e = N_i/2$ (symmetrical membrane). Near equilibrium a linear expansion in n_i of Eq. 60 yields, after some algebra,

$$\frac{1}{2}\frac{dn_i}{dt} = -\frac{l_i K_i P}{2A} n_i + \frac{l_i K_i P N_i}{4AB} \sum_j l_j K_j n_j. \tag{61}$$

A and B correspond to the quantities defined in Eq. 58 by inserting the equilibrium amounts of the lipids. To calculate the phenomenological parameters, we relate the right-hand side of Eq. 61 to the expression

$$J_i^{pass} = -2RT\left(\kappa_i n_i + N_i \sum_j \lambda_{ij} n_j\right). \tag{62}$$

The latter formula follows from linearization of Eq. 44 as well as from neglecting the mechanical forces. One obtains for the phenomenological parameters

$$\kappa_i = \frac{l_i}{4RT}\frac{K_i}{A} P, \quad \lambda_{ij} = -\frac{1}{8RT}\frac{l_i l_j}{k_{eff}}\frac{K_i K_j}{A^2} P, \tag{63a,b}$$

where k_{eff} denotes an effective rate constant of the carrier defined as follows:

$$k_{eff} = \frac{1}{P}\left(kP^0 + \sum_i l_i P_i\right). \tag{64}$$

P^0 and P_i denote the total equilibrium amounts of the unloaded carrier form and loaded carrier forms, respectively, that is, $P^0 = P/A$ and $P_i = P^0 K_i N_i/2$.

Combining Eq. 42 with Eq. 63 yields for the phenomenological coefficients

$$L_{ij} = \frac{P}{4RT}\left[\delta_{ij} l_j \frac{K_j N_j}{A} - \frac{1}{2}\frac{l_i l_j}{k_{eff}}\frac{K_i K_j N_i N_j}{A^2}\right]. \tag{65}$$

Equations 63–65 show that the phenomenological coefficients resulting from a special kinetic equation are in accordance with the general structure given in Eq. 42.

The following properties of the coupling parameters of the antiport mechanism are worth mentioning: 1) The phenomenological parameters in Eqs. 63a,b are proportional to the total amount of the carrier P. 2) The diffusion parameters κ_i as well as the cross-coupling parameters λ_{ij} ($i \neq j$)

and the self-coupling parameters λ_{ii} are proportional to the respective rate constants l_i and l_j of the translocation of the carrier. 3) All coupling parameters λ_{ij} are negative, which reflects that a driving force X_i giving rise to a diffusion flux of species i is accompanied by a cross-coupled flux as well as a self-coupled flux in the opposite direction. 4) The quantity A in the denominators of Eqs. 63 and 65 reflects a saturation of the carrier with lipids. For very low affinities of the lipids for the carrier $K_iN_i \ll 1$, the quantity A tends to unity, that is, saturation effects are negligible. 5) The coupling parameters λ_{ij} are inversely related to the effective rate constant k_{eff} of the carrier. In the case that the unloaded form of the carrier moves much faster than the loaded forms ($k \gg l_i$), the λ_{ij} tend to zero, that is, the fluxes become uncoupled. In the opposite limit $k \to 0$, it follows from Eq. 65 that $L_{ii} = -\Sigma_{j\neq i}L_{ij}$. In this case one row of the matrix of phenomenological coefficients becomes linearly dependent on the other rows. Such a matrix is no longer positive definite, because at least one of its eigenvalues vanishes. Because principles of irreversible thermodynamics require that the matrix L_{ij} is positive definite, vanishing unloaded flip-flop ($k = 0$) is excluded. For example, in the special case of one component ($s = 1$), it is easily verified that diffusion and self-coupling coefficients cancel out in the limit $k \to 0$. Because any nonequilibrium state is accompanied by entropy production, such a situation of vanishing flux is forbidden.

Similar to the scaling properties in Eq. 44a,b derived for the phenomenological parameters of the thermodynamic model, the parameters 63a,b of the kinetic models must be homogeneous functions of all quantities involving units of amounts. Rescaling of the system by a factor α necessitates in the case of carrier mechanisms not only a change of lipid amounts $N_i^{c,e} \to \alpha N_i^{c,e}$, but also of the total amount $P \to \alpha P$ of carrier molecules as well as of the binding constants $K_i \to \alpha^{-1}K_i$.

Symport mechanism. A carrier with two identical lipid-binding sites will be able to translocate single molecules of the various lipid species as well as different pairs of molecules. Making assumptions analogous to those in the case of an antiport, one derives as a kinetic equation of such a symport mechanism:

$$\frac{dN_i^c}{dt} = -\frac{dN_i^e}{dt} = J_i^{pass} = -\frac{2PK_i}{A^cB^e + A^eB^c}(l_i^+N_i^cB^e - l_i^-N_i^eB^c) - \frac{2P}{A^cB^e + A^eB^c}\sum_j K_iK_j(l_{ij}^+N_i^cN_j^cB^e - l_{ij}^-N_i^eN_j^eB^c). \quad (66)$$

The quantities A and B are defined in analogy to Eq. 58, that is,

$$A^{c,e} = \left(1 + \sum_j K_jN_j^{c,e}\right)^2, \quad B^{c,e} = k^{+,-} + 2\sum_j l_j^{+,-}K_jN_j^{c,e} + \sum_{i,j} l_{ij}^{+,-}K_iK_jN_i^{c,e}N_j^{c,e}. \quad (67a,b)$$

In the derivation of these equations, it has been assumed that the two binding sites of the carrier have identical properties. Furthermore, the binding constants are assumed to be layer independent, that is, $K_i^c = K_i^e = K_i$. The factors 2 on the right-hand side of Eq. 66 arise for combinatorial reasons. In the first term this factor reflects that each lipid i may bind to the unloaded carrier at two different binding sites. The factor 2 in the second term corresponds, for $i \neq j$, to the two different forms of the carrier loaded with lipid i and lipid j, whereas for $i = j$ this factor takes into account that two molecules of lipid i are transported in one translocation step. In Eq. 67a the exponent 2 occurs because the two identical binding sites are assumed to be independent. Near equilibrium a linear approximation of Eqs. 66 and 67a,b leads for a symmetrical parameter choice $l_i^{+,-} = l_i$, $l_{ij}^{+,-} = l_{ij}$, and $k^{+,-} = k$ to an equation that may be directly compared with Eq. 62. In this way the coupling parameters are identified as

$$\kappa_i = \frac{P}{2RT}\frac{K_i}{A}\left(l_i + \frac{1}{2}\sum_j l_{ij}K_jN_j\right) \quad (68a)$$

$$\lambda_{ij} = \frac{P}{4RT}\frac{K_iK_j}{A}l_{ij} - \frac{P}{2RT}\frac{K_iK_j}{A^2}\frac{1}{k_{eff}}\left(l_i + \frac{1}{2}\sum_k l_{ik}K_kN_k\right)\cdot\left(l_j + \frac{1}{2}\sum_k l_{jk}K_kN_k\right), \quad (68b)$$

where

$$k_{eff} = \frac{1}{P}\left(kP^0 + \sum_k l_kP_k + \sum_{k,m} l_{km}P_{km}\right). \quad (69)$$

A and B are obtained from Eqs. 67a,b by inserting the equilibrium amounts of the lipids. P^0, P_k, and P_{km} denote the total equilibrium amounts of the unloaded carrier form, the forms loaded with one lipid of species j, and the double loaded forms of the carrier, respectively.

Compared to the parameters of the antiport, the following features of the phenomenological parameters of the symport are remarkable: 1) A coupling parameter λ_{ij} may become positive in case in which the corresponding double-loaded carrier is translocated ($l_{ij} \neq 0$). The sign of the coupling parameters depends crucially on the value of the effective rate constant k_{eff} defined in Eq. 69. If k_{eff} is much higher than all translocation rate constants l_i, l_j, and l_{ij}, then one obtains $\lambda_{ij} > 0$ for all i, j. This can be achieved, for example, if the translocation rate constant k of the unloaded carrier is high enough. 2) The negative term in λ_{ij} in Eq. 68b is

closely related to the diffusion parameters κ_i and κ_j, because it is proportional to their product.

Inclusion of mechanical effects

A translocation of lipid molecules will generally be accompanied by a change in the mechanical energy of both monolayers. This energy change will affect the free energy barriers determining the rate constants of translocation of the loaded carrier forms. As an example, we consider the kinetic equation (Eq. 60) of the antiport mechanism. The energy change ΔE_i for the translocation of Δy_i moles of species i, leading to a change of n_i by $2\Delta y_i$, may be approximated by $(\partial E/\partial y_i)\Delta y_i$. For 1 mole of translocated lipids, this expression reduces, according to Eq. 24, to

$$\Delta E_i \approx \frac{\partial E}{\partial y_i} = -X_i^{\text{mech}}. \tag{70}$$

Assuming a linear profile of the mechanical energy along the translocation coordinate as well as a symmetrical energy barrier in the absence of mechanical stresses, the rate constants obey the following relation:

$$l_i^{\pm} = l_i \exp\left(\mp \frac{X_i^{\text{mech}}}{2RT}\right). \tag{71}$$

Taking into account these expressions in the rate equation (Eq. 60) as well as in the terms $B^{c,e}$ defined in Eq. 58b, the mechanical forces are included in the kinetic model.

The question arises whether this kind of kinetic description is consistent with the thermodynamic flux-force relationships used to obtain Eq. 45. For the comparison of the two approaches, the kinetic rate equation, obtained by combination of Eqs. 60 and 71, as well as the phenomenological flux equation (Eq. 45) must be linearized in the deviations n_i. The linearized kinetic equation reads

$$J_i^{\text{pass}} = \frac{dN_i^c}{dt} = \frac{1}{2}\frac{dn_i}{dt} = \frac{PK_i l_i}{4RTA}\sum_j\left(\delta_{ij} - \frac{N_i}{2B}K_j l_j\right) \cdot (-2RTn_j + N_j X_j^{\text{mech}}). \tag{72}$$

Linearization of Eq. 45 yields

$$J_i^{\text{pass}} = -\sum_j(\delta_{ij}\kappa_j + \lambda_{ij}N_i)(2RTn_j - N_j X_j^{\text{mech}}), \tag{73}$$

which is an extension of Eq. 62 by inclusion of mechanical forces. A comparison of these two equations shows that near equilibrium the kinetic model that includes mechanical forces may be characterized by the same phenomenological parameters as a model that does not contain any mechanical effects (see Eq. 63).

These results support our previous assumption that in the framework of thermodynamic flux-force relations, a unique set of coupling parameters exists, that is, that the entropic and mechanical forces are additive. The incorporation of mechanical forces in the rate constants of the kinetic model may give, therefore, a good representation also of the nonlinear kinetic equation system in Eq. 60. The given procedure has been applied also for the symport mechanism discussed above, with the result that the coupling parameters given in Eqs. 68a,b remain unchanged if the mechanical forces are included in the rate constants (Frickenhaus and Heinrich, unpublished results).

SIMULATIONS

General remarks

The theory outlined in the previous sections is applied to the transversal lipid distribution of the human red blood cell membrane. Time-dependent changes as well as steady states are calculated by means of numerical integration of the differential equations resulting from the thermodynamic and from the kinetic approach for passive fluxes. We take into account the five abundant lipids, phosphatidylserine, phosphatidylethanolamine, phosphatidylcholine, sphingomyelin, and cholesterol (see Zachowski, 1993). The lipid specifying indices $i = 1, \ldots, s$ with $s = 5$ refer to PS, PE, PC, SM, and Ch, respectively.

For the simulations we use the system equations 2. J_i^{pass} is represented either by Eq. 45 (thermodynamic model) or by a kinetic equation resulting from a carrier mechanism (Eq. 60 or 66). An expression for the active fluxes J_i^{act}, which also appears in Eq. 2, is derived below. Furthermore, we have to specify the units of the model quantities.

For the active transport we refer to the result of Seigneuret and Devaux (1984), that there exists in plasma membranes of eukaryotic cells an ATP-dependent carrier that specifically translocates PS and PE from the external to the cytoplasmic leaflet. A simple kinetic expression for this process is obtained under the following assumptions: 1) fast and competitive binding of PS and PE to the translocase on both sides of the membrane, 2) unidirectional transport of PS and PE to the cytoplasmic layer under consumption of one ATP per transported aminophospholipid (Beleznay et al., 1993), and 3) bidirectional flip-flop of the unloaded carrier form. The kinetic equations for the active transport of PS and PE read

$$J_{PS}^{\text{act}} = \frac{l_{PS}^{+}k^{-}T\cdot K_{PS}^{e}N_{PS}^{e}}{D}, \quad J_{PE}^{\text{act}} = \frac{l_{PE}^{+}k^{-}T\cdot K_{PE}^{e}N_{PE}^{e}}{D}, \tag{74a,b}$$

where

$$D = k^{-}(1 + K_{PS}^{e}N_{PS}^{e} + K_{PE}^{e}N_{PE}^{e}) + (k^{+} + l_{PS}^{e}K_{PS}^{e}N_{PS}^{e} + l_{PE}^{e}K_{PE}^{e}N_{PE}^{e})(1 + K_{PS}^{c}N_{PS}^{c} + K_{PE}^{c}N_{PE}^{c}). \tag{74c}$$

In these equations T denotes the total translocase concentration, $K_{PS}^{c,e}$ and $K_{PE}^{c,e}$ are the binding constants of the lipids to the translocase, $k^{+,-}$ are the flip-flop rate constants of the unloaded translocase, and l_{PS}^{+} and l_{PE}^{+} are the effective rate constants of the unidirectional translocations for a fixed

ATP concentration. We leave out a detailed derivation of Eq. 74, because it is easily done by the procedure explained above for the passive carrier mechanisms. In fact, Eq. 74 is formally a special case of the kinetic expression in Eq. 60. However, in the case of active transport, the principle of detailed balance, which would exclude irreversible steps within a translocation cycle, is not relevant because of the coupling to ATP consumption. For a derivation of Eq. 74, see also Heinrich et al. (1997).

Rate constants in the kinetic equations of passive and active carrier mechanisms have units of min^{-1}. Binding constants, which also enter the kinetic models, are usually given in units of mM^{-1}. To meet this choice, the lipid amounts must be expressed in concentration units (mM). For that, we normalize the lipid amounts with respect to a fixed reference volume. A convenient choice is the volume of the red cell as a reference, because it is independent of the cell suspension volume. Of course, the fixed reference volume could be chosen differently, e.g., the bilayer membrane volume, which would rescale only the numerical values of the concentration-dependent system parameters. Furthermore, we use concentration units for the quantities P and T of two of the types of carriers; thus the fluxes are expressed in mM min^{-1}. Concerning the thermodynamic model equations, rescaling of concentrations will affect the unit of the flux, but not the unit of the thermodynamic forces (cf. Eqs. 12, 25, and 45). The diffusion parameters κ_i and coupling parameters λ_{ij}, which enter the phenomenological coefficients, have, according to their original definitions, units of $\mathrm{min}^{-1}\,\mathrm{J}^{-1}$ and $\mathrm{min}^{-1}\,\mathrm{J}^{-1}\,\mathrm{mol}^{-1}$, respectively. Both parameters may be rescaled in such a way that they have the dimension of rate constants. This leads to $\kappa_i' = 4RT\kappa_i$ for the diffusion parameters and to $\lambda_{ij}' = 4NRT\lambda_{ij}$ for the coupling parameters, where N denotes the total concentration of lipids, i.e., $N = \Sigma_i N_i$. In both expressions the factor 4 arises from the linearization of the system equations (Eq. 45) in the vicinity of equilibrium.

Simulations with a reference set of parameters

As a reference model, a set of differential equations (Eq. 2) with passive fluxes from the thermodynamic model (Eq. 45) is considered. The whole set of parameters is reduced in such a way that the model is still able to reproduce certain experimental data for human erythrocytes. In Eq. 45 the area parameters a_i are assumed to be equal, that is, $a_i = a$. For the phenomenological coefficients Eq. 53 is applied, where the coupling parameters are unspecific ($\lambda_{ij} = \lambda = va^2$). Simulations with a more detailed parameter specification are given in the next sections.

Fig. 1 shows time-dependent changes in the lipid concentration ratios N_i^c/N_i as well as the fraction of the total lipid concentration N^c/N in the cytoplasmic layer. The curves are obtained by numerical integration of the system equations, using the parameter values listed in Table 1. The initial state at $t = 0$ is symmetrical, that is, $N_i^c/N_i = 1/2$. For $t < 10{,}000$ min, active translocation for PS and PE takes place, whereas for $t > 10{,}000$ min this translocation is fully inhibited. In the first time interval the lipid concentrations tend toward a steady state, which shows a pronounced asymmetry between the two monolayers. After inhibition of the translo-

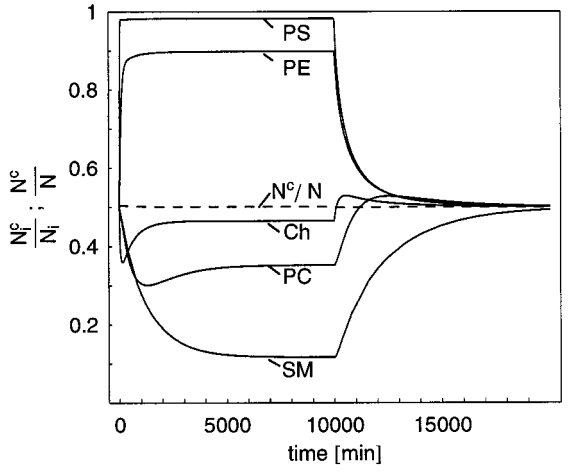

FIGURE 1 Time-dependent changes of the cytoplasmic concentration ratios of the five membrane components for active aminophospholipid translocase ($0 < t < 10{,}000$ min) and for inactive translocase ($t > 10{,}000$ min). Initial and final distributions correspond to the symmetrical equilibrium state of the model. The curves are obtained by numerical integration of system equations 2 by taking into account Eqs. 46 and 76a–c and using parameter values given in Table 1.

TABLE 1 Parameters for the simulation of the reference model

Total lipid concentrations* (mM)	
N_{PS}	0.55
N_{PE}	1.12
N_{PC}	1.24
N_{SM}	1.04
N_{Ch}	3.5
Aminophospholipid translocase‡	
$l_{PS}^+ = l_{PE}^+$	2.0×10^4 min^{-1}
$k^+ = k^-$	4.0×10^4 min^{-1}
$(K_{PS}^e)^{-1} = (K_{PE}^e)^{-1}$	1.0×10^3 mM
$(K_{PE}^e)^{-1}$	0.5 mM
$(K_{PS}^e)^{-1}$	5.0 mM
T	5.5×10^{-6} mM
Phenomenological parameters, molecular areas, and mechanical force constants	
$4N\,RT\,\lambda_{ij}$	1/670 min^{-1}§
$4\,RT\,\kappa_{PS}$	1/600 min^{-1}#a
$4\,RT\,\kappa_{PE}$	1/600 min^{-1}#a
$4\,RT\,\kappa_{PC}$	1/1000 min^{-1}#b
$4\,RT\,\kappa_{SM}$	1/4000 min^{-1}#
$4\,RT\,\kappa_{Ch}$	1 min^{-1}#
γ_i/L_A	0.25 J m^{-2}¶
a_i	0.6 nm^2¶

*From Luly (1989), with a reference volume of erythrocytes of 107 $\mu\mathrm{m}^3$; cf. Heinrich et al. (1997).

#See Heinrich et al. (1997). (a) Lyso-PS: Bergmann et al. (1984). (b) Middelkoop et al. (1986).

§See text and Fig. 2.

¶For determination from experimental data, see text.

case at $t = 10{,}000$ min, the membrane relaxes to equilibrium, which is characterized by symmetric distributions of its components.

The concentration ratios within the asymmetrical steady state and the corresponding experimental data are given in Table 2. It is seen that the model explains rather well the experimentally observed state of the membrane. In particular, it predicts an accumulation of PS and PE on the cytoplasmic layer and a compensating displacement of the other lipids to the external layer. Moreover, the model correctly describes SM as displaced to a greater extent than PC. Taking into account the parameter values from Table 1, it is observed that the slowest diffusing component SM reaches the most pronounced asymmetry, whereas cholesterol shows a nearly symmetrical distribution due to its fast passive translocation.

Fig. 1 and Table 2 show that within the whole time range, the sum of lipid concentrations is well balanced between the two monolayers ($N^c \approx N^e$), despite strong changes in the concentrations of the individual membrane components. In an initial phase (for ~100 min) the inward translocation of PS and PE is mainly compensated by the displacement of cholesterol. Within the subsequent phase there are also significant displacements of PC and SM.

The results of the simulation depend crucially on the value of the coupling parameter λ. This is demonstrated in Fig. 2, where the normalized steady-state concentrations are plotted as functions of λ. Simulations are possible only for such values of λ, for which L_{ij} is a positive definite matrix, that is, for $\lambda > \lambda_c$ (see text below Eq. 53). Using the shift $\lambda \rightarrow \lambda - \lambda_c$ allows for a logarithmic display of the abscissa in Fig. 2. It is observed that at $\lambda = 0$ the steady-state ratios N_i^c/N_i are the same for those species that are translocated only passively. This property can be derived analytically by taking into account that for vanishing cross-couplings the steady-state condition for the species PC, SM, and Ch, that is, for $i = 3$, 4, and 5, simplifies to $X_i^{entr} + X_i^{mech} = 0$. Because for $a_i = a$ the mechanical forces X_i^{mech} are independent of i, it follows directly from Eq. 45 that the steady-state ratios N_i^c/N_i become species independent as well. Crossing the value $\lambda = 0$ leads to a qualitative change in the lipid distribution. For $\lambda < 0$ one obtains $N_{Ch}^c/N_{Ch} < N_{PC}^c/N_{PC} < N_{SM}^c/N_{SM}$, whereas $\lambda > 0$ leads to the reverse situation, $N_{SM}^c/N_{SM} < N_{PC}^c/N_{PC} < N_{Ch}^c/N_{Ch}$. The experimental data (Table 2) are strongly in favor of the latter case, which means that a positive coupling parameter λ is realistic. The point $\lambda = \lambda^*$ in Fig. 2 indicates the reference parameter choice used in Table 1 with the corresponding simulation in Fig. 1. In view of the scattering of the experimental data, one may conclude from Fig. 2 that λ-values higher than the reference value could be justified as well.

TABLE 2 Steady-state lipid distribution of the reference model compared to experimental data

	Lipid Concentration Ratios					
	Experimental Data					Theoretical
	a	b	c	d	e	(Fig. 1)
N_{PS}^c/N_{PS}	1.0	0.81	0.92	1.0	—	0.98
N_{PE}^c/N_{PE}	0.95	—	0.79	0.80	0.82	0.89
N_{PC}^c/N_{PC}	0.45	0.30	0.28	0.24	0.44	0.35
N_{SM}^c/N_{SM}	0.15	—	0.21	0.18	—	0.12
N_{Ch}^c/N_{Ch}	—	—	—	—	—	0.47

a, Dressler et al. (1984); b, Haest et al. (1978); c, VanMeer et al. (1981); d, Verkleij et al. (1973); e, Williamson et al. (1982).

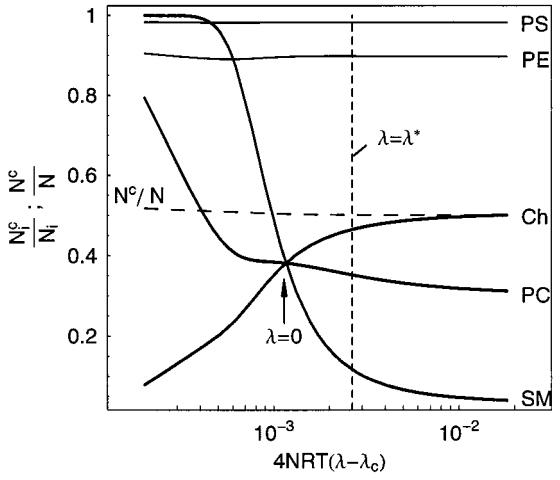

FIGURE 2 Steady-state concentration ratios of the five lipids (——) and their total normalized cytoplasmic concentration (– – –) as functions of scaled cross-coupling parameter λ. λ_c denotes the lower bound of λ for positive definiteness of the matrix of phenomenological coefficients (L_{ij}), using the parameters from Table 1 ($4NRT\lambda_c = -1.163 \times 10^{-3}$ min^{-1}). The arrow points to the crossing point of the curves for PC, SM, and Ch, obtained for $\lambda = 0$. The vertical dotted line indicates the value of λ used for the simulations shown in Fig. 1 with the corresponding steady-state concentrations listed in Table 2.

Simulation with different force constants and equilibrium areas

It has been demonstrated for stearoyloleoylphosphatidylcholine (SOPC) bilayer vesicles and for extracts of red blood cell membranes that an increasing cholesterol mole fraction is accompanied by an increase in the elastic area compressibility modulus K (Needham and Nunn, 1990). To analyze the composition-dependent effects on mechanical properties, it is necessary to choose lipid-specific compression force constants γ_i in the present model.

Defining an effective force constant as

$$\gamma_{eff} = \frac{\sum_j N_j a_j}{\sum_k N_k a_k/\gamma_k}, \tag{75}$$

the mechanical energy from Eq. 23 may be rewritten as

$$E = \frac{1}{4}\gamma_{eff}\frac{(\Delta A)^2}{A_0}, \tag{76}$$

where the definition of ΔA in Eq. 26 is used. $A_0 = \frac{1}{2}\Sigma_j N_j a_j$ denotes the total equilibrium bilayer area. Formula 76 may be directly compared with the expression

$$E = \frac{k_r}{2A_0}\left(\frac{\Delta A}{h}\right)^2, \tag{77}$$

which has been used previously to define the nonlocal bending modulus k_r (cf. Svetina and Žekš, 1992); h denotes the distance between the two monolayer neutral surfaces and is approximately half the bilayer thickness (Waugh et al., 1992). Note that in Eq. 77 the energy unit is Joule and not Joule mol^{-1}. From Eqs. 76 and 77 one obtains

$$\gamma_{eff} = 2\frac{k_r}{h^2} L_A. \tag{78}$$

k_r and γ_{eff} are related to the experimentally accessible compressibility modulus K by $k_r = h^2K/4$ (cf. Svetina and Žekš, 1992; Waugh et al., 1992) for a symmetrical planar bilayer, and thus $\gamma_{eff} = L_AK/2$.

Expression 75 may be simplified by taking into account the experimental fact that variations in the mole fractions of different phospholipid components have a minor influence on K (Evans and Needham, 1987). This suggests considering the force constants and the surface areas of the phospholipids PS, PE, PC, and SM as unspecific parameters γ_{PL} and a_{PL}, respectively. Then the effective force constant defined in Eq. 75 may be expressed as a function of the cholesterol mole fraction $x = N_{Ch}/N$ as follows:

$$\gamma_{eff} = \frac{xa_{Ch} + (1-x)a_{PL}}{xa_{Ch}/\gamma_{Ch} + (1-x)a_{PL}/\gamma_{PL}}. \tag{79}$$

A similar formula has been taken into account for SOPC vesicle membranes (Needham and Nunn, 1990) for the dependence of K on the fraction of lipid-cholesterol complexes and the uncomplexed lipids. Equation 79 may be rewritten in terms of the molecular area ratio $r_a = a_{PL}/a_{Ch}$ and the force constant ratio $r_\gamma = \gamma_{PL}/\gamma_{Ch}$:

$$\gamma_{eff} = \gamma_{PL}\frac{x + (1-x)r_a}{xr_\gamma + (1-x)r_a} = \gamma_{PL} f(x). \tag{80}$$

$f(x)$ increases monotonically with x for $r_\gamma < 1$ and decreases monotonically for $r_\gamma > 1$. Obviously γ_{eff} reduces to γ_{PL} for $x = 0$ and to γ_{Ch} for $x = 1$.

The bilayer elastic modulus K has been measured for red blood cell membrane extracts for $x = 0.4$ and $x = 0.8$ (Needham and Nunn, 1990). The ratio of the two moduli $K(0.8)/K(0.4) = 783/423 = 1.85$ may be used to determine the ratio of the force constants. With the lipid areas $a_{PL} = 0.65$ nm^2 and $a_{Ch} = 0.37$ nm^2 (cf. Needham and Nunn, 1990), that is, $r_a = 1.76$, one obtains with Eq. 80 a ratio $r_\gamma = 0.16$. This combination of parameters corresponds to the thick solid line for $f(x)$ in Fig. 3 (*curve a*). The thin solid lines (*b*, *c*, and *d*) represent $f(x)$ for $r_a = 1.76$ and different r_γ values. The dashed line (*e*) represents the hypothetical case $r_a < 1$.

With $r_a = 1.76$ and $r_\gamma = 0.16$, the value of γ_{PL} may be determined from the experimental value $K = 423$ dyn cm^{-1} for $x = 0.4$, using again Eq. 80 and the relation $\gamma_{eff} = L_AK/2$. This yields $\gamma_{PL}/L_A = 0.163$ J m^{-2}, which corresponds to a modulus of $K = 325$ dyn cm^{-1} for the cholesterol-free membrane. The latter parameter is a factor 2.2 above the measured value for dimyristoylphosphatidylcholine (DMPC) (cf. Evans and Needham, 1987). It is noteworthy that the parameter fit leading to curve *a* in Fig. 3 qualitatively reproduces the very recent measurements of the cholesterol dependence of the bending modulus k_{cp} of phospholipid bilayers (Chen and Rand, 1997). The experimental values of $k_{cp}(0.3)/k_{cp}(0) \approx 1.15$ for dioleoylphosphatidylethanolamine and $k_{cp}(0.5)/k_{cp}(0.2) \approx 1.22$ for dioleoylphosphatidylcholine (see Figure 10 in Chen and Rand, 1997) are roughly in agreement with $f(0.3)/f(0) = 1.19$ and $f(0.5)/f(0.2) = 1.28$, respectively. From these considerations and the experimental value for the intact red blood cell $K = 500$ dyn cm^{-1} (Katnik and Waugh, 1990), the parameter $\gamma_{eff}/L_A = 0.25$ J m^{-2} is derived, corresponding to a nonlocal bending modulus $k_r = 2 \times 10^{-18}$ J (for $h = 4$ nm). The values, presented in Table 3, for γ_{eff}, a_{PL}, a_{Ch}, and r_γ lead via Eq. 75 to $\gamma_{PL}/L_A = 0.18$ J m^{-2} and $\gamma_{Ch}/L_A = 1.12$ J m^{-2}. These area and force constant ratios are used for the simulation of the time-dependent transbilayer lipid distribution shown in Fig. 4. The coupling parameters $\lambda_{ij} = va_ia_j$ are calculated with $4NRTva^2 = 1.49 \times 10^{-3}$ min^{-1}, where a is the arithmetical mean of the area parameters. With the values of a_{Ch} and a_{PL} for PS, PE, PC, and SM, mentioned above, one obtains $a = 0.594$ nm^2, which corresponds to the areas a_i used in the reference simulation (see Table 1 and Fig. 1).

The time-dependent changes shown in the inset of Fig. 4 are very similar to the corresponding curves in Fig. 1. In

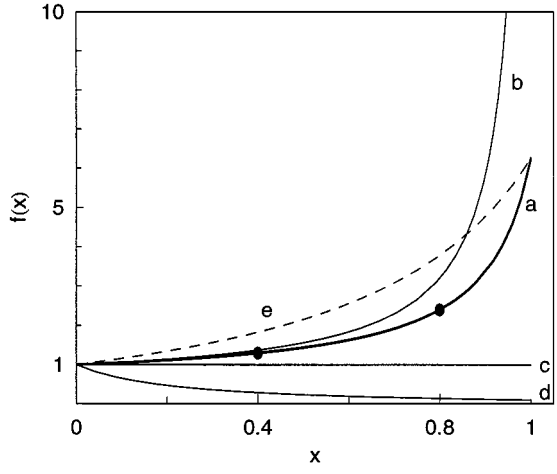

FIGURE 3 $f = \gamma_{eff}/\gamma_{PL}$ as a function of cholesterol mole fraction x for different parameters. (*a*) $r_a = 1.76$, $r_\gamma = 0.16$. (*b*) $r_a = 1.76$, $r_\gamma = 0.01$. (*c*) $r_a = 1.76$, $r_\gamma = 1.0$. (*d*) $r_a = 1.76$, $r_\gamma = 10.0$. (*e*) $r_a = 1/1.76$, $r_\gamma = 0.16$. The thick solid line *a* is for model parameters $a_{Ch} = 0.37$ nm^2 and $a_{PL} = 0.65$ nm^2, which lead to $r_\gamma = 0.16$ to fit the indicated experimental points for $x = 0.4$ and $x = 0.8$ (Needham and Nunn, 1990).

TABLE 3 Parameters for simulations using the symport model

$l_{PS} = l_{PE}$	70 min^{-1}
l_{PC}	30 min^{-1}
l_{SM}	10 min^{-1}
l_{Ch}	3×10^4 min^{-1}
l_{ij}	250 min^{-1}
k	4×10^4 min^{-1}
$K_i^{e-1} = K_i^{e-1}$	50 mM
P	6×10^{-4} mM
γ_{eff}/L_A	0.25 J m^{-2}
a_{PL}	0.65 nm^2
a_{Ch}	0.37 nm^2
r_γ	0.16

particular, this concerns the extent of asymmetry of the lipid distributions in the steady state. There are, however, slight modifications brought about by the differentiation between the areas of cholesterol and those of the other lipids. This is indicated by the differences $\Delta_i = N_i^c/N_i - (N_i^c/N_i)_{ref}$ and the corresponding difference Δ for the total cytoplasmic lipid concentrations shown in Fig. 4. It is observed that, in the lipid-specific case, cholesterol remains, shortly after activation of PS- and PE-transport, closer to its equilibrium distribution, that is, $\Delta_{Ch} > 0$, whereas PC and SM exhibit a stronger asymmetry ($\Delta_{PC} < 0$, $\Delta_{SM} < 0$). This effect of parameter changes for the molecular areas is easily understood by the facts that 1) smaller a_{Ch} values decrease the cross-coupling parameters for cholesterol, and 2) the mechanical forces are lowered for cholesterol because $X_i^{mech} \propto a_i$. In a similar way it can be understood that PC and SM show a more pronounced response if their area parameters are increased. Reducing the area parameter of cholesterol means that in the outer layer more phospholipids are present for balancing the total areas of both of the leaflets. This explains why N^c/N decreases compared to the reference model ($\Delta < 0$; Fig. 4).

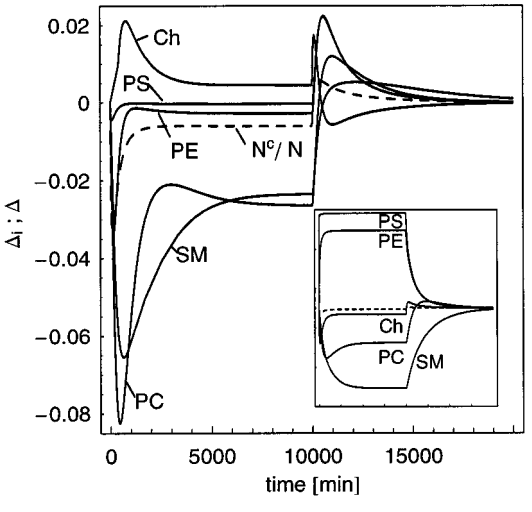

FIGURE 4 Time-dependent changes of lipid concentration ratio differences for a set of parameters with lipid-specific areas and lipid-specific force constants. Δ_i and Δ denote the deviations of cytoplasmic concentration ratios N_i^c/N_i and N^c/N, respectively, between this simulation and the reference simulation (Fig. 1). The molecular surface areas are $a_{PL} = 0.65$ nm^2 and $a_{Ch} = 0.37$ nm^2. The force constants are $\gamma_{PL}/L_A = 0.18$ J m^{-2} and $\gamma_{Ch}/L_A = 1.123$ J m^{-2}, yielding with Eq. 77 $\gamma_{eff}/L_A = 0.25$ J m^{-2}, which corresponds to the lipid-unspecific γ-value in Table 1. For the cross-coupling parameters λ_{ij}, the area-dependent expression 52 has been used with $v > 0$ (see text). The inset shows the time-dependent changes of the cytoplasmic concentrations of the five membrane components (scaling of the axes as in Fig. 1).

Simulation with a carrier mechanism for the passive fluxes

The calculations presented in the previous two sections have indicated that a simulation of the experimental data concerning the asymmetrical steady state of the membrane requires positive coupling parameters. For that reason we use in the following the symport mechanism introduced above, which, in contrast to the antiport mechanism, may give rise to $\lambda_{ij} > 0$ for certain parameter combinations. Concerning the inclusion of mechanical forces, we use Eq. 71 for the rate constants of the singly loaded carrier forms. For the double loaded forms the expression

$$l_{ij}^{\pm} = l_{ij} \exp\left(\mp \frac{X_i^{mech} + X_j^{mech}}{2RT} \right) \tag{81}$$

is applied by considering the energy differences of a simultaneous translocation of two lipid molecules i and j.

Figs. 5 and 6 show the time-dependent changes simulated on the basis of the symport carrier. The curves are obtained by integration of the system 2 of differential equations by

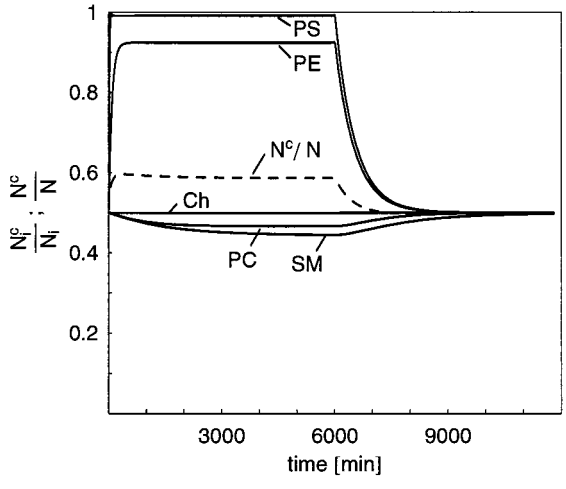

FIGURE 5 Time-dependent changes of the cytoplasmic concentration ratios of the five membrane components for active aminophospholipid translocase ($0 < t < 10{,}000$ min) and for inactive translocase ($t > 10{,}000$ min). The curves are obtained by numerical integration of the system equations 2, using for passive translocation a symport carrier as explained in the text, excluding mechanical forces, and for active translocation Eqs. 74a–c. Parameter values for total lipid concentrations and for active translocase are given in Table 1. For the parameter values of the symport carrier, see Table 3.

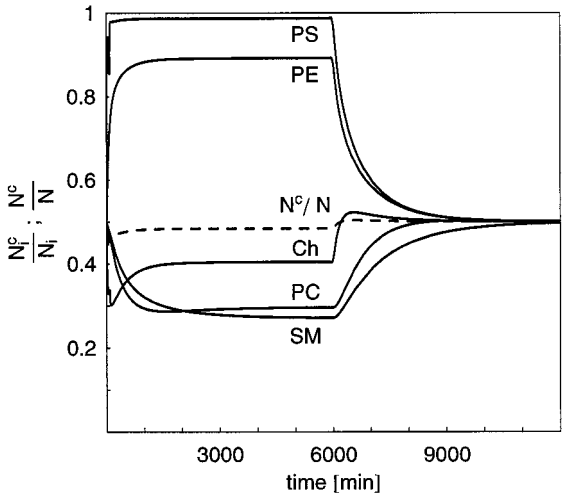

FIGURE 6 Time-dependent changes of the cytoplasmic concentration ratios of the five membrane components for active aminophospholipid translocase ($0 < t < 10{,}000$ min) and for inactive translocase ($t > 10{,}000$ min). The curves are obtained by numerical integration of the same equations and parameters used for Fig. 5, with the exception that the effect of mechanical forces on the rate constants of the symport carrier are included (see text and Eqs. 71 and 81). The values for a_{PL}, a_{Ch}, γ_{PL}, and γ_{Ch} are given in the legend to Fig. 4.

taking into account Eq. 66 for the passive transport and Eq. 74 for the active transport.

For Fig. 6, Eqs. 71 and 81 for the rate constants have been applied. As parameters of the passive carrier the values listed in Table 3 were used. The total amounts of the lipids as well as the parameters of the active translocase are taken from Table 1. It is seen from Fig. 5 that neglecting the mechanical forces yields a stationary distribution of lipids that deviates strongly from the experimental result. In particular, the species PC and SM, which are translocated only passively, show in these simulations an almost negligible asymmetry. As a consequence, the total lipid amounts are not well balanced (see the *dashed line* in Fig. 5). An inclusion of mechanical forces leads to a considerable improvement of the simulation results, as demonstrated in Fig. 6. In particular, the pattern of asymmetry is qualitatively correct, and the total lipid amounts are well balanced. However, the asymmetry of sphingomyelin is too low compared to the experimental outcome (see Table 2).

The parameter values in Table 3 have been adjusted in such a way that they give diffusion parameters κ_i, according to Eq. 68a, on the same order of magnitude as the values that have been applied for the reference simulation (see Table 1). The question arises whether the predicted value for the steady-state asymmetry of SM may be improved compared to the result shown in Fig. 6, for example, by decreasing the rate constants associated with translocation of SM, which would lower the corresponding κ_{SM} value (see discussion of Fig. 1). However, this possibility is ruled out, as can be seen from inspection of Eq. 68b. Lower $l_{SM,j}$ values yield, by necessity, smaller cross-coupling parameters $\lambda_{SM,j}$. This does not allow for a pronounced asymmetry of SM, as has been shown in Fig. 2 for the reference model. In this way the parameter choice for the rate constants involving SM (Table 3) represents a compromise allowing for a rather slow carrier-mediated diffusion by keeping the cross-coupling strong enough.

Fig. 7 shows the time course of the ratios $l_i^+/l_i^- = \exp(-X_i^{mech}/RT)$ during the response of the system depicted in Fig. 6. The curves illustrate that the effects of the mechanical forces on the carrier kinetics are strongest in the initial phase after activation of the translocase where PS and PE are accumulated in the inner leaflet. It is observed that the subsequent redistribution of the other membrane components diminishes these effects to a certain level. The activity of the translocase results in nonvanishing mechanical forces in the stationary state, such that the ratio of the rate constants l_i^+ and l_i^- amounts to 2.0 for phospholipids and 1.5 for cholesterol. The difference between these two numbers is due to the different molecular surface areas (see Table 3). The effect of mechanical forces on the rate constants of cholesterol translocation is smaller because its area parameter is reduced by a factor of 0.57 compared to the phospholipids. The ratio l_i^+/l_i^- equal to unity is obtained only after relaxation toward equilibrium if the translocase is fully inhibited. Similar results are obtained for the effect of mechanical forces on the ratios l_{ij}^+/l_{ij}^- of the rate constants of the doubly loaded forms of the carrier.

DISCUSSION

The present paper gives a theoretical investigation of the dynamic state of cellular membranes, particularly of the transversal distribution of lipid components. The asymmetrical state of the bilayer arises primarily from the activity of

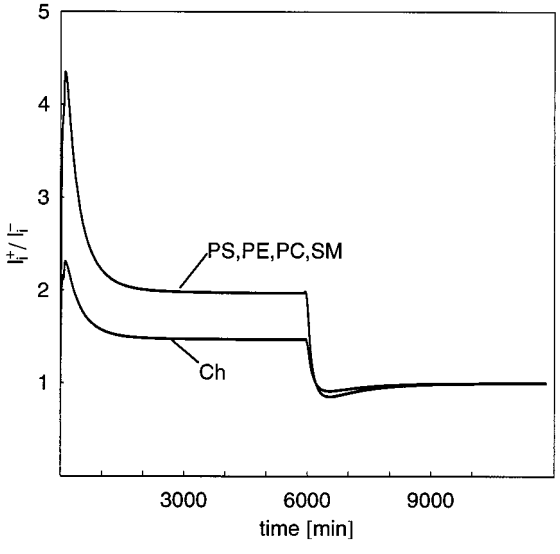

FIGURE 7 Time-dependent changes of the ratios l_i^+/l_i^- of kinetic constants of the symport model after activation ($0 < t < 10{,}000$ min) and inhibition ($t > 10{,}000$ min) of the translocase. The curves reflect the effect of mechanical forces on the kinetics of the symport carrier during the time course displayed in Fig. 6.

an ATP-dependent aminophospholipid transporter. Focusing the analysis on the passive response to this active transport, it is shown that a sufficient mathematical description necessitates a detailed analysis of different forces arising in states of nonequilibrium distribution of the membrane components. Two different approaches are presented for the modeling of passive transversal movements. The first makes use of linear flux-force relations of near-equilibrium thermodynamics and includes entropic and mechanical effects. The second approach is based on kinetic models.

Simulations with the thermodynamic approach yield a rather good quantitative agreement with experimental data for the distribution of the five main lipid components of erythrocyte plasma membrane, provided that a positive cross-coupling of lipid-specific fluxes is taken into account. In the framework of kinetic modeling we have used a symport mechanism of passive translocation, because antiport mechanisms do not provide positive cross-coupling parameters.

In the kinetic models the mechanical forces are taken into account, for the first time, by their effects on the activation barriers of the passive translocation step. Neglecting mechanical effects leads to strong imbalances in the total lipid amounts between the monolayers. However, the simulations with a symport agree only qualitatively with the experiments, even after inclusion of mechanical effects. Discrepancies, mainly with respect to the transversal distribution of sphingomyelin in erythrocytes, may not be removed within the assumed symport mechanism by a simple adjustment of the model parameters, as has been shown by inspection of the interrelation between cross-coupling parameters and diffusion parameters (cf. discussion of Eq. 68). From this one may conclude that the detailed kinetic mechanism of passive translocation deserves further theoretical investigation. For example, it is attractive to analyze kinetic models of diffusion through narrow pores or inverted micelles. Preliminary results of corresponding kinetic models show that a sequential ordering of lipids along the translocation coordinate (and thus sequential lipid translocation) should also yield positive cross-couplings, whose values may be sufficiently high, even with low diffusion parameters (S. Frickenhaus and R. Heinrich, unpublished results).

In the present work the model is used primarily for simulation of steady-state lipid asymmetries. Our conclusion that a positive cross-coupling of passive lipid fluxes occurs should be also tested in transient states, for example, by modeling the time-dependent redistribution of fluorescence/spin-labeled lipids. Bitbol and Devaux (1988) and Connor et al. (1992) measured an ATP dependence of the rate constants of passive outward movement of labeled lipids. Both investigations indicated that the aminophospholipid translocase operation enhances the outward motion of phospholipids. Our model is able to explain such an effect on the basis of a positive coupling: The active inward translocation of PS and PE is accompanied by their passive movement in the counterdirection. Consequently, the outward movement of other phospholipids is enhanced by a positive coupling to the passive outward movement of PS and PE. Simulations of experimental protocols of labeled lipid experiments thus may be used to go beyond the steady-state test of our model by quantifying the mediated ATP dependence of outward passive movement.

Active transport has been modeled on the basis of a kinetic scheme, involving competitive binding of phosphatidylserine and phosphatidylethanolamine. It is clear that besides the kinetic parameters of passive translocation, those of the active transport are affected by mechanical forces. However, the presented mechanism of the active transport is not detailed enough to allow for a proper treatment of mechanical effects, because ATP binding, ATP hydrolysis, ADP release, and lipid translocation are lumped into single irreversible translocation steps for PS and PE. Despite its simplicity, the proposed equations for active translocation are compatible with the present knowledge about the kinetic properties of active lipid translocation in erythrocytes. This concerns, in particular, the competition of PS and PE for the same binding site, with a 10-fold higher affinity of PS on the external monolayer (Zachowski et al., 1986). The latter property results in a pronounced difference in the time constants of active transport of these two lipids (Bitbol and Devaux, 1988). Of course, one could develop more elaborate models of active translocation. For example, the inclusion of an ATP-dependent compensatory lipid movement from the cytoplasmic to the external side, which has been proposed by Bitbol and Devaux (1988) and Connor et al. (1992), would be an interesting extension of the presented work.

The present analysis not only gives a model for simulation of experimental data, concerning the transmembrane exchange of lipids, but also yielded new theoretical insights, which are of relevance to the description of other membrane transport systems. We could give, for example, a profound derivation of the structure of the expressions for coupling coefficients of passive membrane transport, mainly with respect to their dependence on the total amounts of the transported substances. It may be of general theoretical importance that we were able to give quantitative cross-relations between a thermodynamic model and a kinetic description. In this way we could take advantage of two kinds of theoretical approaches, which are usually considered to be rather distinct.

The phenomenological coefficients, which appear in the thermodynamic approach, may result from different kinetic mechanisms operating independently. As an example, besides carrier mediated transport, one could take into account in the kinetic description a protein independent lipid flip-flop (Kornberg and McConnell, 1971). The corresponding phenomenological coefficients of each mechanism are then additive quantities, and the contribution of each mechanism can be analyzed separately.

It is worth mentioning that the phenomenological coefficients derived by linearization of the kinetic equations of lipid transport do not contain terms involving molecular area parameters. In particular, terms proportional to $a_i a_j$,

which appear in the coefficients derived from mechanism independent thermodynamic arguments (see Eq. 53), are not present in the corresponding expressions resulting from the kinetic description of translocation. This may be seen by comparison of Eq. 53 with Eq. 65 for the antiport mechanism, taking into account that the latter equation for the phenomenological coefficients also holds true after inclusion of mechanical effects. It remains an open question whether a mechanistic interpretation may be given for the terms proportional to $a_i a_j$ appearing in the phenomenological model.

The effect of proteins on membrane asymmetry has been taken into account in the mechanism of active translocation and, in the kinetic approach, in the mechanism of facilitated lipid transport. However, possible effects of the mechanical properties of the membrane proteins have not been analyzed in detail. This may be an oversimplification in view of the fact that a rather high portion of the membrane surface (~50% for erythrocytes) is occupied by proteins. It would be straightforward to extend expression 13 for the mechanical energy of the monolayers by incorporating compressible protein components. This would lead to a modified formula for the mechanical forces, which contains, compared to Eq. 25, additional terms proportional to $N_p a_p/\gamma_P$ in the denominator, where the index P refers to proteins. Accordingly, expression 75 for the effective force constant is then extended by the same terms in the denominator, and by terms proportional to $N_P a_P$ in the numerator. In the realistic case, where proteins have a higher force constant than the effective force constant of the protein free lipid membrane, γ_{eff} will be increased by taking proteins into account. For the simulations presented above we have used for γ_{eff} a value derived from experimental data for the red blood cell membrane (Needham and Nunn, 1990). Thus the net effect of proteins on the mechanical force constants was taken into account, at least qualitatively.

Besides mechanical forces, transmembrane electric potential gradients may also affect the translocation kinetics of lipids, depending on their ionization states under physiological conditions. From a theoretical point of view, the corresponding model extensions would not be too difficult as long as the transmembrane potential as well as the surface potentials are considered to be fixed. A more realistic approach would necessitate the calculation of the electrical forces as functions of the local charges, which are dependent on the transversal lipid distribution, the ionic strength on both sides of the membrane, as well as the out-of-plane orientation of polar headgroups. In this way the present model deserves extensions from various experimental and theoretical approaches, including, for example, molecular dynamics simulations. However, there are experiments indicating that changes of the external surface potential as well as of the transmembrane potential have a negligible effect on the passive transbilayer movement of phospholipids in human red blood cells (Jänchen et al., 1996).

The present model neglects effects of lateral organization of cell membranes that could result from specific lipid-lipid interactions, for example, the pronounced interaction of cholesterol and sphingomyelin (Bittman et al., 1994), as well as protein-lipid interactions. In principle, these interactions would give rise to a more general expression for the free energy of mixing. Preliminary results, based on the Bragg-Williams approximation (cf. Hill, 1960), indicate that no qualitative changes concerning the simulation of the overall transversal lipid distributions occur, at least in the limits of that approximation (Schilling et al., unpublished results).

The expressions for the mechanical forces have been derived under the simplifying assumption that in states of asymmetrical composition the membrane remains planar. The question may arise of how the model is modified by effects of membrane curvature. In a first approach, a time-independent area difference ΔA^{curv} due to curvature between the two monolayers may be introduced in Eq. 14 with $A_0^{c,e} = A_0 \pm \Delta A^{curv}/2$. In the latter ansatz, the quantity A_0 represents the surface area of the planar membrane surface. Performing analogous calculations as for the planar membrane, the resulting expression 25 for the mechanical forces is modified in a simple way: the area difference ΔA^{curv} is subtracted from $\Delta A = \Sigma n_j a_j$. Obviously, such a modification shifts the mechanical equilibrium state of the membrane from a planar to a curved shape. These considerations may serve as a first step in developing a steady-state model that accounts for effects of cell shape on lipid asymmetry. In a longer perspective one could think of models describing in a combined way time-dependent membrane shapes and transmembrane asymmetry-generating processes, such as active lipid transport.

We are very grateful to A. Herrmann, P. Müller, and I. Bernhardt (Humboldt University, Berlin) as well as M. Brumen (University Maribor, Slovenia) for fruitful discussions and helpful comments on the manuscript. An anonymous reviewer is acknowledged for very valuable hints.

REFERENCES

Beleznay, Z., A. Zachowski, P. F. Devaux, M. Puente Navazo, and P. Ott. 1993. ATP-dependent aminophospholipid translocation in erythrocyte vesicles: stoichiometry of transport. *Biochemistry.* 32:3146–3152.

Bergmann, W. L., V. Dressler, C. W. M. Haest, and B. Deuticke. 1984. Reorientation rates and asymmetry of distribution of lysophospholipids between the inner and outer leaflet of the erythrocyte membrane. *Biochim. Biophys. Acta.* 772:328–336.

Bitbol, M., and P. F. Devaux. 1988. Measurement of outward translocation of phospholipids across human erythrocyte membrane. *Proc. Natl. Acad. Sci. USA.* 85:6783–6787.

Bittman, R., C. R. Kasireddy, P. Mattjus, and J. P. Slotte. 1994. Interaction of cholesterol with sphingomyelin in monolayers and vesicles. *Biochemistry.* 33:11776–11781.

Blau, L., and R. Bittman. 1978. Cholesterol distribution between the two halves of the lipid bilayer of human erythrocyte ghost membranes. *J. Biol. Chem.* 253:8366–8368.

Brasaemle, D. L., A. D. Robertson, and A. D. Attie. 1988. Transbilayer movement of cholesterol in the human erythrocyte membrane. *J. Lipid Res.* 29:481–489.

Bretscher, M. S. 1972. Phosphatidyl-ethanolamine: differential labeling in intact cells and cell ghosts of human erythrocytes by a membrane-impermeable reagent. *J. Mol. Biol.* 71:523–528.

Brumen, M., R. Heinrich, A. Herrmann, and P. Müller. 1993. Mathematical modeling of lipid transbilayer movement in the human erythrocyte plasma membrane. *Eur. Biophys. J.* 22:213–223.

Chen, Z., and R. P. Rand. 1997. The influence of cholesterol on phospholipid membrane curvature and bending elasticity. *Biophys. J.* 73: 267–276.

Connor, J., C. H. Pak, R. F. A. Zwaal, and A. J. Schroit. 1992. Bidirectional transbilayer movement of phospholipid analogs in human red blood cells. *J. Biol. Chem.* 27:19412–19417.

de Groot, S. R., and P. Mazur. 1962. Nonequilibrium Thermodynamics. North-Holland, Amsterdam.

Devaux, P. F. 1991. Static and dynamic lipid asymmetry in cell membranes. *Biochemistry.* 30:1163–1173.

Dressler, V., C. W. M. Haest, G. Plasa, B. Deuticke, and J. D. Erusalimsky. 1984. Stabilizing factors of phospholipid asymmetry in the erythrocyte membrane. *Biochim. Biophys. Acta.* 755:189–196.

Evans, E., and D. Needham. 1987. Physical properties of surfactant bilayer membranes: thermal transitions, elasticity, rigidity, cohesion, and colloidal interactions. *J. Phys. Chem.* 91:4219–4228.

Gordesky, S. E., and G. V. Marinetti. 1973. The asymmetric arrangement of phospholipids in the human erythrocyte membrane. *Biochem. Biophys. Res. Commun.* 50:1027–1031.

Haest, C. W. M., G. Plasa, D. Kamp, and B. Deuticke. 1978. Spectrin as stabilizer of the phospholipid asymmetry in the erythrocyte membrane. *Biochim. Biophys. Acta.* 509:21–32.

Heinrich, R., M. Brumen, A. Jaeger, P. Müller, and A. Herrmann. 1997. Modeling of phospholipid translocation in the erythrocyte membrane: a combined kinetic and thermodynamic approach. *J. Theor. Biol.* 185: 295–312.

Heinrich, V., S. Svetina, and B. Žekš. 1993. Nonaxisymmetric vesicle shapes in a generalized bilayer-couple model and the transition between oblate and prolate axisymmetric shapes. *Phys. Rev. E.* 48:3112–3123.

Hill, T. L. 1960. Introduction to Statistical Thermodynamics. Addison-Wesley, Reading, MA.

Jänchen, G., J. Libera, T. Pomorski, P. Müller, A. Herrmann, and I. Bernhardt. 1996. The influence of external surface potential and transmembrane potential on the passive transbilayer movement of phospholipids in the red blood cell membrane. *Gen. Physiol. Biophys.* 15: 415–442.

Katnik, C., and R. Waugh. 1990. Alterations of the apparent expansivity modulus of the red blood cell membrane by electric fields. *Biophys. J.* 57:877–882.

Kornberg, R. D., and H. M. McConnell. 1971. Inside-outside transitions of phospholipids in vesicle membranes. *Biochemistry.* 10:1111–1120.

Lange, Y., and J. M. Slayton. 1982. Interaction of cholesterol and lysophosphatidylcholine in determining red cell shape. *J. Lipid Res.* 23: 1121–1123.

Luly, P. 1989. Membrane lipid changes in the abnormal red cell. *In* The Red Cell Membrane. A Model for Solute Transport. B. U. Raess and G. Tunnicliff, editors. Clifton: Humana Press, Clifton, NJ. 399–421.

Middelkoop, E., B. H. Lubin, J. A. F. Op den Kamp, and B. Roelofsen. 1986. Flip-flop rates of individual molecular species of phosphatidylcholine in the human red cell membrane. *Biochim. Biophys. Acta.* 855:421–424.

Needham, D., and S. R. Nunn. 1990. Elastic deformation and failure of lipid bilayer membranes containing cholesterol. *Biophys. J.* 58: 997–1009.

Schroeder, F., G. Nemecz, G. W. Wood, C. Joiner, G. Morrot, M. Ayraut-Jarrier, and P. F. Devaux. 1991. Transmembrane distribution of sterol in the human erythrocyte. *Biochim. Biophys. Acta.* 1066:183–192.

Schultz, S. G. 1980. Carrier mediated transport. *In* Basic Principles of Membrane Transport. Cambridge University Press, Cambridge.

Seifert, U., K. Berndl, and R. Lipowsky. 1991. Shape transformations of vesicles: phase diagram for spontaneous curvature and bilayer-coupling models. *Phys. Rev. A.* 44:1182–1202.

Seigneuret, M., and P. F. Devaux. 1984. ATP-dependent asymmetric distribution of spin-labeled phospholipids in the human erythrocyte membrane: relation to shape changes. *Proc. Natl. Acad. Sci. USA.* 81:3751–3755.

Sheetz, M. P., and S. J. Singer. 1974. Biological membranes as bilayer couples. A mechanism of drug-erythrocyte interactions. *Proc. Natl. Acad. Sci. USA.* 71:4457–4461.

Svetina, S., and B. Žekš. 1989. Membrane bending energy and shape determination of phospholipid vesicles and red blood cells. *Eur. Biophys. J.* 17:101–111.

Svetina, S., and B. Žekš. 1992. The elastic deformability of closed multilayered membranes is the same as that of a bilayer membrane. *Eur. Biophys. J.* 21:251–255.

VanMeer, G., C. G. Gahmberg, J. A. F. Op den Kamp, and L. L. N. Van Deenen. 1981. Phospholipid distribution in human En(a-) red cell membranes which lack the major sialoglycoprotein glycophorin A. *FEBS Lett.* 135:33–55.

Verkleij, A. J., R. F. A. Zwaal, B. Roelofson, P. Comfurius, D. Castelijn, and L. L. M. van Deenen. 1973. The asymmetric distribution of phospholipids in the human red cell membrane. *Biochim. Biophys. Acta.* 323:178–193.

Waugh, R. E., J. Song, S. Svetina, and B. Žekš. 1992. Local and nonlocal curvature elasticity in bilayer membranes by tether formation from lecithin vesicles. *Biophys. J.* 61:974–982.

Williamson, P., J. Bateman, K. Kozarsky, K. Mattocks, N. Hermanovicz, H.-R. Choe, and R. A. Schlegel. 1982. Involvement of spectrin in the maintenance of phase-state asymmetry in the erythrocyte membrane. *Cell.* 30:725–733.

Zachowski, A. 1993. Phospholipids in animal eukaryotic membranes: transverse asymmetry and movement. *Biochem. J.* 294:1–14.

Zachowski, A., E. Favre, S. Cribier, P. Hervé, and P. F. Devaux. 1986. Outside-inside translocation of aminophospholipids in the human erythrocyte membrane is mediated by a specific enzyme. *Biochemistry.* 25:2585–2590.

Zachowski, A., P. Fellman, and P. F. Devaux. 1985. Absence of transbilayer diffusion of spin-labeled sphingomyelin in human erythrocytes. Comparison with the diffusion of several spin-labeled glycerophospholipids. *Biochim. Biophys. Acta.* 815:510–514.